PID-Type Fuzzy Control for Anti-Lock Brake Systems with Parameter Adaptation*

Chih-Keng CHEN** and Ming-Chang SHIH***

In this research, a platform is built to accomplish a series of experiments to control the Antilock Brake System (ABS). A commercial ABS module controlled by a controller is installed and tested on the platform. The vehicle and tire models are deduced and simulated by a personal computer for real time control. An adaptive PID-type fuzzy control scheme is used. Two on-off conversion methods: pulse width modulation (PWM) and conditional on-off, are used to control the solenoid valves in the ABS module. With the pressure signal feedbacks in the caliper, vehicle dynamics and wheel speeds are computed during braking. Road surface conditions, vehicle weight and control schemes are varied in the experiments to study braking properties.

Key Words: PWM, Fuzzy Control, Adaptive, ABS System, Hydraulic System

1. Introduction

Anti-lock Braking System (ABS) is an important development in vehicle safety in recent years. When a vehicle is under emergency braking, the ABS can prevent the wheels from skidding and the vehicle from spinning. Thus, the vehicle can be kept under desired control and, in some circumstances, it can shorten the vehicle's braking distance. With the hydraulic pressure regulator in the system, it can reduce the braking oil pressure and retain appropriate rolling of the tire. In most passenger cars, ABS has become a mature product and standard safety equipment. Even for motorcycles, ABS has found its applications to maintain the braking force and vehicle stability(2).

When the vehicle is running, ground forces acting on the tire are shown in Fig. 1. Ground forces include the normal force F_z, the longitudinal force F_x and the lateral force F_y. F_z comes from the weight and load of the vehicle. Its magnitude also changes due to the load transfer effect during braking. The longitudinal force F_x is produced during driving and braking. The lateral force F_y helps the vehicle in turning and maneuvering, or in some cases, in resisting a side disturbance force such as the wind.

The reduction in braking distance depends on whether F_x can be maintained at its maximum value. During braking, the contact patch between tire and ground begins to slip. This substantially affects both the longitudinal and lateral friction coefficients. The well known parameter to represent slippage is the slip ratio. The tire slip ratio is defined as:

$$S = \frac{V_v - V_\omega}{V_v} = \frac{V_v - R\omega}{V_v} \tag{1}$$

where V_v is the absolute vehicle speed, $V_\omega = R\omega$ is the wheel speed, R is the effective radius of the wheel, ω is the angular speed of the wheel. From the definition, one can conclude that when $S = 0$ the wheel is in perfect rolling motion without slipping. On the other hand, when $S = 1$ the wheel is locked and pure sliding happens. The slip ratio greatly affects the longitudinal and lateral forces. The

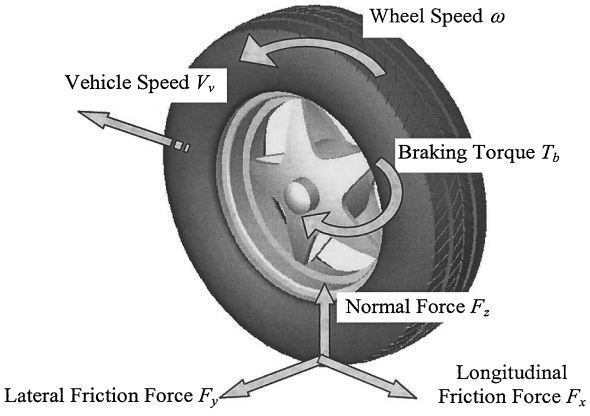

Fig. 1 Free body diagram of a single wheel

* Received 22nd July, 2003 (No. 03-5085)

** Department of Mechanical Engineering, National Cheng Kung University, Tainan 701, Taiwan

*** Department of Mechanical and Automation Engineering, Da-Yeh University, Changhua 515, Taiwan, ROC.
E-mail: ckchen@mail.dyu.edu.tw

models for the friction coefficients and slip ratio are investigated by experiments[3] and described in mathematical equations[1),(9)]. The relations of the friction coefficients (μ_x and μ_y respectively for longitudinal and lateral friction coefficients) and the slip ratio S are shown in Fig. 2[3)]. During braking, in addition to the longitudinal force on the tire, the lateral force maintains vehicle stability in a straight or turning motion. Therefore, both longitudinal and lateral forces should be considered to achieve shorter braking distance without losing its maneuverability. From Fig. 2, one can observe that on a dry road surface, the longitudinal friction coefficient increases initially and drops after its peak as the slip ratio increases. The lateral friction coefficient that influences the vehicle maneuverability decreases by the raise of slip ratio. The optimal region to be controlled is around the peak value of μ_x since it can keep the maximum braking force while still maintaining the maneuverability (or μ_y). However the peak value of μ_x may change for different road conditions and vehicle speeds[7]. Therefore, the on-line search for the optimal slip ratio for ABS control is a crucial and challenging problem.

Many control schemes are used in ABS control applications. The describing-function method is applied to the design of ABS systems[4]. The fuzzy model reference learning control (FMRLC) method[5] is used to control the automotive ABS and to optimize the braking effectiveness under adverse road conditions. Mauer (1995)[6] proposes methods to analyze the relation between the braking torque and the slip ratio, and further, to identify road conditions. This way can avoid the excessive slipping of the wheel. Wu, Lee, & Shih[10] apply neural-fuzzy control theory to the design of the ABS controller under the influences of different road surface states. Wu, & Shih[11),(12)] use the sliding-mode PWM scheme in the ABS controller

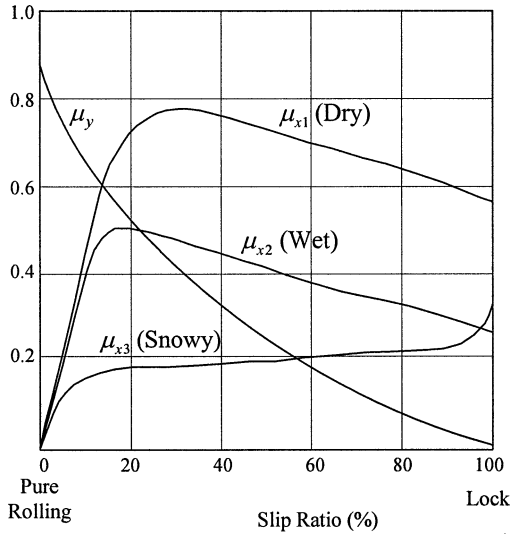

Fig. 2 Relation of longitudinal μ_x and lateral μ_y friction coefficients to slip ratio

design and build the vehicle test bench for both simulation and experiments.

In this study, an adaptive PID-type fuzzy controller is used to control the Antilock Brake System (ABS). Using a commercial ABS pressure regulation unit, a platform is implemented to accomplish a series of experiments. The optimal slip ratios at different road surfaces and vehicle loads are estimated as the reference input. The controller with a parameter-adaptation mechanism is used for the ABS control. The experimental configuration used in this research is designed and discussed in section 2. A simplified vehicle model and tire-road force relations are shown in section 3. Control schemes implemented in the platform are developed in section 4. Experimental results to evaluate ABS performance are presented and discussed in section 5.

2. Experimental Configuration

The schema of the experimental platform used in this study is shown in Fig. 3. On this platform, a hydraulic cylinder is used to simulate the action of the braking pedal pressing on the master cylinder booster. Two outlets from the master cylinder accomplish the X-type braking circuits. A commercial ABS actuator is installed between the master cylinder and the brake calipers on the four wheels. The hydraulic circuit in the ABS actuator is shown in Fig. 4. There are two control valves for each wheel: a normally opened inlet valve and a normally closed outlet valve. In normal operation, high pressure oil flow through the inlet valves and pushes the brake calipers on the disks and, thus the braking torque is built on the wheel. To decrease the pressure, the outlet valve is opened and the inlet valve is closed. To hold the pressure in caliper, both valves are closed to maintain the pressure.

In the experimental configuration as shown in Fig. 3, a pressure sensor is installed to measure the pressure in the caliper and to feed it back to a computer. Control signals are computed and sent to activate the Darlington

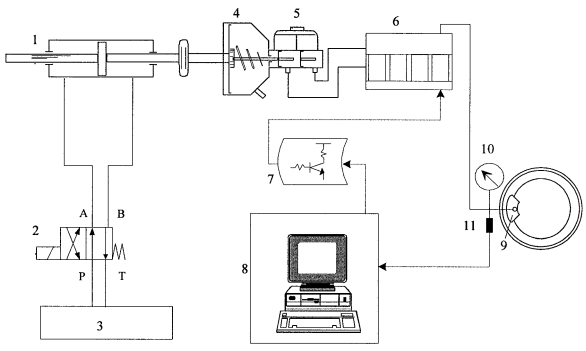

1 Cylinder
2 Directional valve
3 Hydraulic power unit
4 Booster
5 Master cylinder
6 ABS actuator
7 Darlington circuit
8 PC for simulator of vehicle dynamics, tire force and ABS controller
9 Caliper
10 Pressure gauge
11 Pressure transducer

Fig. 3 Schematic of experimental system

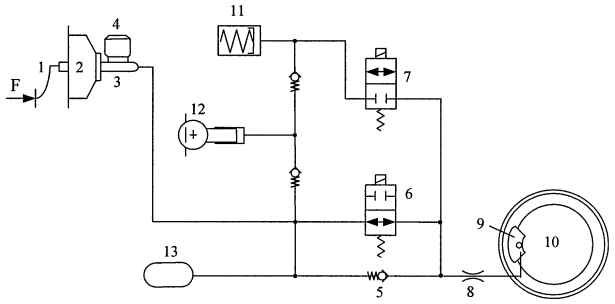

1 Brake pedal
2 Booster
3 Master cylinder
4 Reservoir
5 Check valve
6 Inlet valve
7 Outlet valve
8 Throttle
9 Caliper
10 Brake disk
11 Damper
12 Oil return pump
13 Accumulator

Fig. 4 ABS hydraulic circuit

circuits to control the solenoids and oil-return motor inside the ABS actuator. This platform can be used to study ABS actions and performance for the four wheels. To simplify the model, in this research, only one wheel's braking dynamics is investigated. Vehicle dynamics and braking forces acting on the tire are computed online by a personal computer (PC). After the system starts, the pressure sensor measures the caliper's pressure and thus the braking torque can be obtained. The tire-ground model can be used to determine adhesion forces acting on the tire. To consider the real-time simulation, the vehicle model is simplified to a single wheel system. The ABS control action's basic rule is to release high pressure in the calipers when the wheels are going to be locked during emergency braking. While the wheels regain their rotation, pressure should be retained by driving the return-oil pump in the actuator. The vehicle and tire models are developed and coded in the PC for real-time simulation. Also, ABS controllers are implemented in the same computer to control the system. Detailed procedures are discussed in the following two sections.

3. Tire and Vehicle Models

During braking, vehicle dynamics is affected by the tire-road interactive forces. Accordingly, to evaluate the performance of an ABS system, the tire and vehicle models are developed here for on-line computation.

3.1 Tire model

In this study, the tire model[3] that describes the longitudinal friction force F_t as a function of slip ratio S and vehicle speed V_v is written as:

$$F_t = \begin{cases} \dfrac{C_s \cdot S}{1-S}, \text{ when } \dfrac{C_s \cdot S}{1-S} < \dfrac{\mu \cdot N}{2} \\ N\left[\mu - \mu^2 \dfrac{N(1-S)}{4C_s \cdot S}\right], \text{ when } \dfrac{C_s \cdot S}{1-S} > \dfrac{\mu \cdot N}{2} \end{cases} \quad (2)$$

where C_s is the longitudinal stiffness of the tire, μ is the adhesion coefficient of the tire-road surface and N is the normal force on the tire. According to Dugoff's experimental results, the adhesion coefficient μ on a dry road surface decreases linearly with the increase of slip speed and can be modeled as:

$$\mu = \mu_0(1 - A_s \cdot V_v \cdot S) \quad (3)$$

where μ_0 is the coefficient at the slipless state and A_s is a linear decreasing factor due to slip speed $V_v \cdot S$. On a wet road surface, the coefficient decreases exponentially with the raise of slip ratio and is modeled as:

$$\mu = \mu_0 \cdot \exp\left(-\frac{V_v \cdot S}{V_c}\right) \quad (4)$$

where V_c is the road-surface-property velocity, which is related to the root mean square texture height of the road surface.

3.2 Vehicle model

The vehicle considered in this paper is a simplified single wheel model. During braking, two torques are applied on the wheel, as shown in Fig. 1. The first one is the braking torque generated by increased pressure in the caliper. To simplify the model, the relationship between caliper pressure P_s and the braking torque T_b is assumed to be linear and is written as:

$$T_b = K_b \cdot P_s \quad (5)$$

where K_b is a braking constant. The torque generated by the friction force between tire and road surface is $T_t = F_x \cdot R_w$, where F_x is the friction force from the ground and R_w is the radius of the wheel.

The moment balance equation can be written as:

$$I_w \cdot \dot{\omega} = T_t - T_b = F_x \cdot R_w - T_b \quad (6)$$

Vehicle acceleration is computed by the quarter-vehicle model:

$$a_v = -\frac{F_x}{M_v/4} \quad (7)$$

where M_v is the vehicle mass. The vehicle speed V_v can be computed from the integration of the vehicle acceleration a_v is $V_v = \int a_v dt + V_{v0}$, where V_{v0} is the initial speed, which can be obtained from the wheel speed just before the braking pedal is pressed. By integration again, the braking distance can be written as $X_v = \int V_v dt$.

3.3 Performance enhancement

From the previous discussion, one can see that slip ratio and adhesion coefficients are crucial to ABS control. To increase the performance of the ABS controller, many schemes like slip ratio estimation, optimal slip ratio search and road condition identification can be added to the control algorithms. They are discussed in this section and also implemented in subsequent experiments.

3.3.1 Slip ratio estimation To control the ABS system, one may have to calculate the slip ratio in (1) in real time. However, due to tire slippage, it is difficult to measure the vehicle's absolute velocity V_v on a real road running without expensive sensors. Also, the time delay in the hydraulic system should be considered in the control scheme. Therefore, a slip ratio estimator is designed

Table 1 The average optimal slip ratio at different speed ranges

Speed(km/hr) \ Road Surface	Dry	Wet
100-90	0.2995	0.1300
90-80	0.3170	0.1380
80-70	0.3375	0.1460
70-60	0.3620	0.1560
60-50	0.3940	0.1690
50-40	0.4355	0.1865
40-30	0.4940	0.2110
30-20	0.5850	0.2485

here to predict the slip ratio for feedback control. Rewrite Eq. (1) in the form of:

$$S(t)V_v(t) = V_v(t) - R\omega(t) \tag{8}$$

Differentiate (8) on both sides with respect to time and rearrange it, one has:

$$\dot{S}(t) = \frac{1}{V_v(t)}[(1-S(t))a_v(t) - R\alpha(t)] \tag{9}$$

By first-order approximation to the time derivative of $S(t)$, one has:

$$\dot{S}(t) \approx \frac{S(k+1)-S(k)}{\Delta t} \tag{10}$$

where Δt is the sampling time. The discretized form of Eq. (9) becomes:

$$S(k+1) = S(k) + \frac{\Delta t}{V_v(k)}[(1-S(k))a_v(k) - R\alpha(k)] \tag{11}$$

where $a(k)$ is the angular acceleration computed by the differential of angular speeds, i.e. $a(k) \approx \dfrac{\omega(k)-\omega(k-1)}{\Delta t}$. Equation (11) can be used to predict the slip ratio for the control feedback.

3.3.2 The optimal slip ratio The tire adhesion coefficient μ is dependent of vehicle speed as shown in Eqs. (3) and (4). Therefore, the optimal slip ratio with maximum braking force may vary for different vehicle speeds. To control the wheel and to maintain a maximum braking force, an optimal slip ratio can be computed at different speed ranges. In Table 1, average optimal slip ratios are computed for 8 different speed ranges between 20 and 100 km/hr.

3.3.3 Road condition identification On different road conditions, e.g. dry and wet road, the tire-road surface adhesion coefficients and the optimal slip ratios are also different, as shown in Fig. 2. In this study, acceleration and its change rate are used to infer road conditions. The decision scheme to identify road conditions is shown in Fig. 5. The logic shown initially assumes a wet road. If acceleration (or deceleration) $a_v < -6$, it is assumed a dry road. When the road is dry and the change rate $\dot{a}_v > 2$, then it is assumed the wheel is from dry to wet surface. On the other hand, when the road is wet and the change rate $\dot{a}_v < -2$, it stands from wet to dry surface.

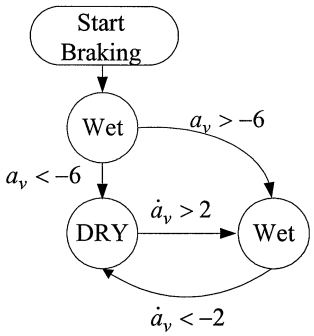

Fig. 5 Scheme for road-surface identification

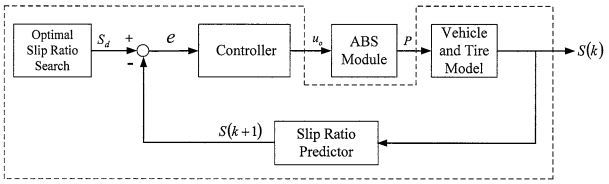

Fig. 6 ABS control block diagram

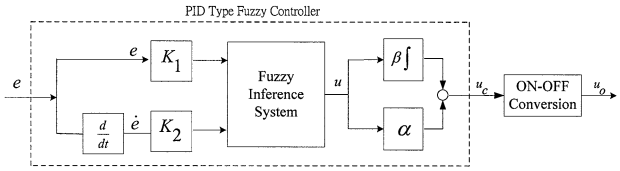

Fig. 7 PID type fuzzy controller and on-off conversion

4. Controller Design

Recently, fuzzy controllers have become popular in many applications due to their simplicity and their intuitive implementations. In this section, the controller design for the ABS system is discussed. The control system block diagram is shown in Fig. 6. Inside the dashed line is the codes implemented on the PC shown in part number 8 of Fig. 3. It includes control scheme, vehicle dynamics and tire force model computed in real time. In the diagram, the slip-ratio is estimated and fed back. The control output is the continuous signal in most controller designs, therefore, the signal conversion from continuous one to on-off action to activate the solenoids in the ABS module is necessary, as shown in Fig. 7. Two on-off conversion schemes are also introduced in this section to compare their performance.

4.1 PID type fuzzy controller

In this study, the fuzzy controller structure is shown in Fig. 7. Its inputs are the slip ratio error e and its change rate $\dot{e}$ and the output u. The variables e and $\dot{e}$ are defined as:

$$\begin{cases} e(k) = S_d - S(k) \\ \dot{e}(k) = \dfrac{S(k)-S(k-1)}{\Delta t} \end{cases} \tag{12}$$

where S_d is the optimal reference slip ratio as defined in Table 1 and $S(k)$ is the estimated slip ratio.

Table 2 Rule table for the fuzzy controller

$\dot{e}$ \ e / u	NB	NM	NS	ZE	PS	PM	PB
NB	-1	-1	-1	$-\frac{2}{3}$	$-\frac{2}{3}$	$-\frac{1}{3}$	0
NM	-1	-1	$-\frac{2}{3}$	$-\frac{2}{3}$	$-\frac{1}{3}$	0	$\frac{1}{3}$
NS	-1	$-\frac{2}{3}$	$-\frac{2}{3}$	$-\frac{1}{3}$	0	$\frac{1}{3}$	$\frac{2}{3}$
ZE	$-\frac{2}{3}$	$-\frac{2}{3}$	$-\frac{1}{3}$	0	$\frac{1}{3}$	$\frac{2}{3}$	$\frac{2}{3}$
PS	$-\frac{2}{3}$	$-\frac{1}{3}$	0	$\frac{1}{3}$	$\frac{2}{3}$	$\frac{2}{3}$	1
PM	$-\frac{1}{3}$	0	$\frac{1}{3}$	$\frac{2}{3}$	$\frac{2}{3}$	1	1
PB	0	$\frac{1}{3}$	$\frac{2}{3}$	$\frac{2}{3}$	1	1	1

The fuzzy subsets of the two antecedent parts e and $\dot{e}$ are denoted as A_i and B_j respectively, where A_i, $B_j \in$ {NB, NM, NS, ZE, PS, PM, PB}. Seven triangular membership functions are used for each variable as shown in Fig. 10. They are symmetrically distributed about the origin, however, are more concentrated between -0.5 and 0.5 to increase the rule-firing sensitivity in this range. The fuzzy control rules are in the form of:

If e is A_i and $\dot{e}$ is B_j then u is u_{ij}

where u_{ij} is a crisp value.

The corresponding fuzzy rules used in this research are listed in Table 2 which are modified from the original one used in Qiao and Mizumoto's study[8]. As proved in their analysis, when the product-sum crisp inference is used, the input-output relation of the controller can be deduced in the form of:

$$u = A + Pe + D\dot{e} \tag{13}$$

where A, P and D are the corresponding coefficients determined from the parameters of the fuzzy system. The controller is called a PD type fuzzy controller (PDfc) since it behaves like a parameters-time-varying PD controller. Further, the scaling factors K_1 and K_2 for e and $\dot{e}$ parts, are also introduced in the controller, the I/O relation in (13) can be rewritten as

$$u = A + PK_1e + DK_2\dot{e} \tag{14}$$

Then, in the control scheme, K_1 and K_2 can be changed in the adaptive mechanism.

Essentially, PDfc may cause a steady state error when applied to control a type zero plant. Therefore, the integral part should be integrated into the fuzzy controller to improve its performance. Qiao and Mizumoto[8] propose a controller structure that simply connects the PD type and the PI type together as shown in Fig. 7. The outcome is called the PID-type fuzzy control scheme that can be written in the following form:

$$\begin{aligned} u_c &= \alpha u + \beta \int u dt \\ &= \alpha(A + PK_1e + DK_2\dot{e}) \\ &\quad + \beta \int (A + PK_1e + DK_2\dot{e}) dt \end{aligned}$$

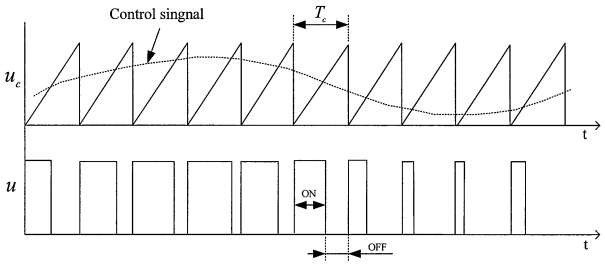

Fig. 8 PWM on-off conversion scheme

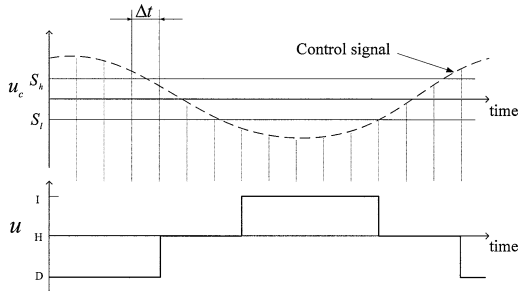

Fig. 9 Conditional on-off conversion scheme

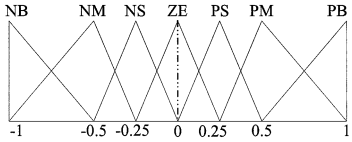

Fig. 10 Membership functions for e and $\dot{e}$

$$\begin{aligned} &= \alpha A + \beta A t + (\alpha K_1 P + \beta K_2 D)e \\ &\quad + \beta K_1 P \int e dt + \alpha K_2 D\dot{e} \end{aligned} \tag{15}$$

where parameters α and β are defined respectively as the weights on PD type and PI type part of the fuzzy controller. This controller is used in the following experiments for ABS control.

4.2 Parameter adaptation

On the one hand, it can be observed that increasing integration part results in more oscillations and instability; on the other hand, reducing it partly may slow down response. Consequently, a parameter-adjust mechanism is necessary to solve the problem. After reexamining Eq. (15) one can discover that the equivalent gains of the corresponding PID control components are the proportional gain $\alpha K_1 P + \beta K_2 D$, integral gain $\beta K_1 P$ and differential gain $\alpha K_2 D$. To reduce the integral gain without changing the proportional gain, the following two tuning rules are proposed[8]:

$$K_2 = \frac{K_{2s}}{\delta_k}, \quad \beta = \delta_k \beta_s \tag{16}$$

where δ_k is the absolute value of the k-th peak error as shown in Fig. 11, and K_{2s} and β_s are the initial values of parameters K_2 and β. In the tuning algorithm (16), a few issues can be pointed out:

1. The integral gain β is decreased by multiplying the

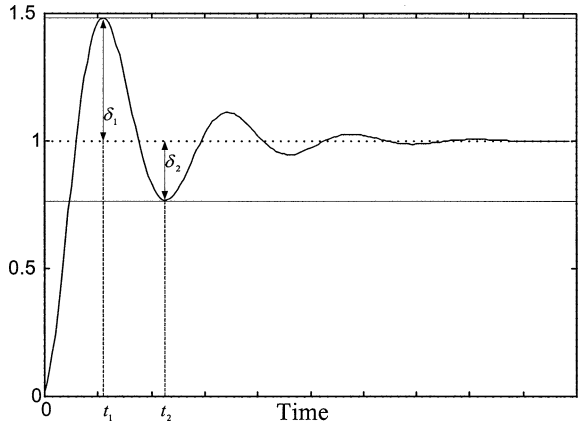

Fig. 11 Step response and peak values

peak error δ_k. As δ_k declines, the integral control component is also decreased to increase system stability.

2. Since value βK_2 is unchanged, the proportional component is maintained at constant, and thus, so is the convergent speed.

3. The gain for the derivative part increases with the decline of the peak error. This can improve relative stability.

The block diagram of the control system can be plotted as shown in Fig. 12,

4.3 PWM on-off conversion

The fuzzy controller output should be converted to the on-off signal to control the solenoid valves in the ABS module. The PWM scheme uses high frequency periodic signals (with period T_c) to be the carrier wave, and determines the duty ratio which is defined as the ratio of "on period" to "off period". In this study, a sawtooth wave is used as the carrier and the duty ratio during one period T_c is determined as shown in Fig. 8. At the "on" period, the inlet valve is opened and the outlet valve is closed as shown in Fig. 4. It can increase the pressure in the caliper and also the braking torque. In contrast, at the "off" time, the inlet valve is closed and the outlet valve is opened to reduce its pressure to prevent the wheel from locking during braking. The solenoid valves are controlled to follow these two different states during the ABS control.

4.4 Conditional on-off conversion

Similar to the PWM conversion scheme, the conditional conversion scheme is also used in converting the continuous signal into a corresponding on-off one. The difference from the PWM is that the basic unit of switch time period is the sampling time Δt while the PWM scheme determines the duty ratio of on and off for the output signal within a sampling period. As shown in Fig. 9, the on-off signal u is determined by two threshold values S_h and S_l which represent the upper and lower bounds of the physical variable to be controlled. Here, in the ABS control application, S_h and S_l are chosen as the two bounds of slip ratio and the conversion rules are defined

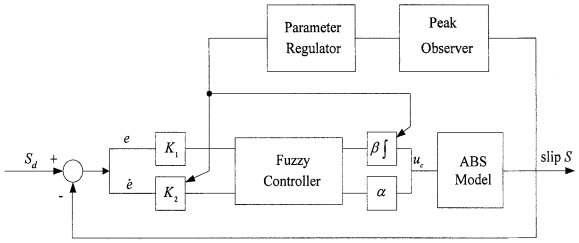

Fig. 12 Block diagram of the adaptive PID-like fuzzy controller[8]

Table 3 Parameters used in experiments

Vehicle Weight	1100 kg
Wheel Radius	0.275 m
Braking Constant K_b	0.001936
Initial Velocity	100 km/hr
Dry Road Parameters	$\mu_0 = 1, C_s = 10F_z, A_s = 0.01$
Wet Road Parameters	$\mu_0 = 0.6, C_s = 10F_z, V_c = 27.8$
Pedal Lever Ratio	4.2
Effective Disk Radius	120mm
Friction Coefficient of Lining	0.35

Table 4 Results without ABS system

	Brake Time(sec)	Brake Distance(m)	Deceleration (m/s^2)
Dry Road	3.61	54.35	7.69
Wet Road	7.89	125.06	3.51

as:

If signal $u_c > S_h$ the output u is off.

If signal $u_c < S_l$ the output u is on.

Otherwise the output status is not changed.

The on-off signal is used to control the solenoids in ABS module. It determines the three control statuses: increase (I), decrease (D) and hold (H), for the braking pressure. All these states can be realized by controlling the inlet and outlet valves in Fig. 4.

5. Experimental Results

In this experimental study, the braking distance and time are investigated from when braking starts to when the vehicle stops without considering the driver's response time. Wheel slip angles are assumed to be zero, that is, only straight running on a uniform flat road surface is studied. Air resistance, aerodynamics and suspension vibrations are neglected. Parameters used in the following experiment studies are listed in Table 3. Initial speed is chosen as 100 km/hr and then, the cylinder in Fig. 3 is activated to push the booster for braking. The system sampling time Δt is set to 0.02 sec. For the case that ABS is not enabled, the vehicle brakes from 100 km/hr initial speed. Braking time, braking distance and vehicle deceleration are computed on dry and wet road surfaces, respectively,

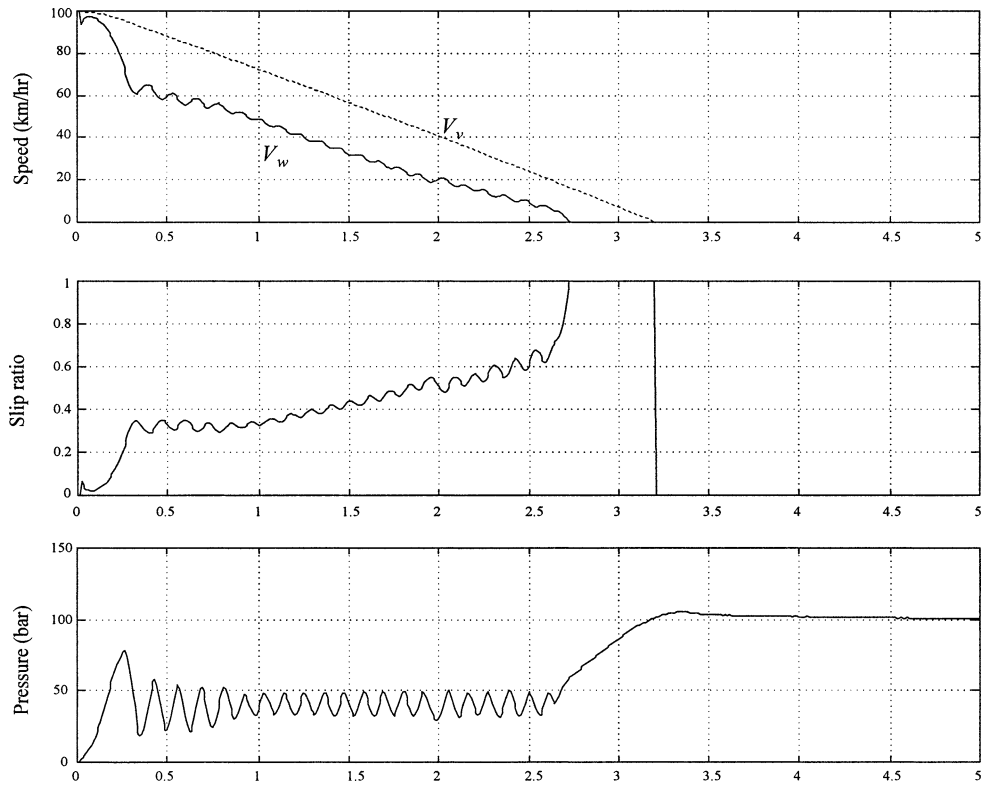

Fig. 13 Results of Fuzzy-PWM control on dry road surface

Table 5 Results by PID FUZZY-PWM control with parameter adaptation

	Brake Time(sec)	Brake Distance(m)	Deceleration (m/s^2)
Dry Road	3.20	46.68	8.68
Wet Road	5.60	80.87	4.96
Dry to Wet	4.55	57.87	6.11
Wet to Dry	3.82	61.63	7.27

as shown in Table 4. These data are compared with the following cases. Different control methods and parameters are used in different experiment cases and results are compared and discussed.

5.1 Fuzzy control with PWM conversion

In this case, the PID type fuzzy controller with adaptive mechanism introduced in section 4.2 is used to control the ABS system on different road conditions. The controller output is converted into on-off commands by the PWM scheme to control the solenoids in ABS module. The ABS controller is tested on four different road surfaces: dry, wet, dry to wet and wet to dry. Experimental results are shown in Table 5. Compared with the results without ABS (data in Table 4), braking time and distance in Table 5 are effectively reduced and decelerations are increased in each corresponding road condition. The time response of the experiment on dry road is shown in Fig. 13. In the speed plot, V_v and $V_w = R\omega$ denote vehicle speed and wheel speed respectively. As braking begins, it is initially assumed to be on the wet road and the desired slip ratio is smaller than the one on a dry road. When pressure in the caliper increases, the controller detects the vehicle's deceleration on a dry road and then changes the optimal reference for the dry road. One can observe that the slip ratio increases as the vehicle speed decreases. This is due to the optimal slip ratio raising when vehicle speed declines, as shown in Table 1. When vehicle speed is lower than 20 km/hr, ABS is disabled and the brake system returns to its normal function even if the wheel is locked. Figure 14 shows control results when the wheel brakes on dry to wet road surface. One can observe the transition between the two road conditions (from 1.5 sec to 2 sec). The controller detects the sudden increase in slip ratio and decrease in vehicle deceleration and thus switches the desired slip ratio from dry to wet side as in Table 1. Therefore, the ABS system shows its ability in reducing the braking distance and avoiding wheel lock. And thus, the maneuverability of the vehicle is also preserved.

5.1.1 Effect of parameter adaptation The parameter adaptation introduced in section 4.2 is used in the previous control experiments. Theoretically, adding the scheme to the controller may raise the ability to track the desired reference and reduce the effects of parameter variations. When this parameter adjustment is disabled, the same experiment is carried out for comparison. The results without adaptation are shown in Table 6. When compared with Table 5, it can be seen that in Table 6 the braking time and distance are longer for each corresponding

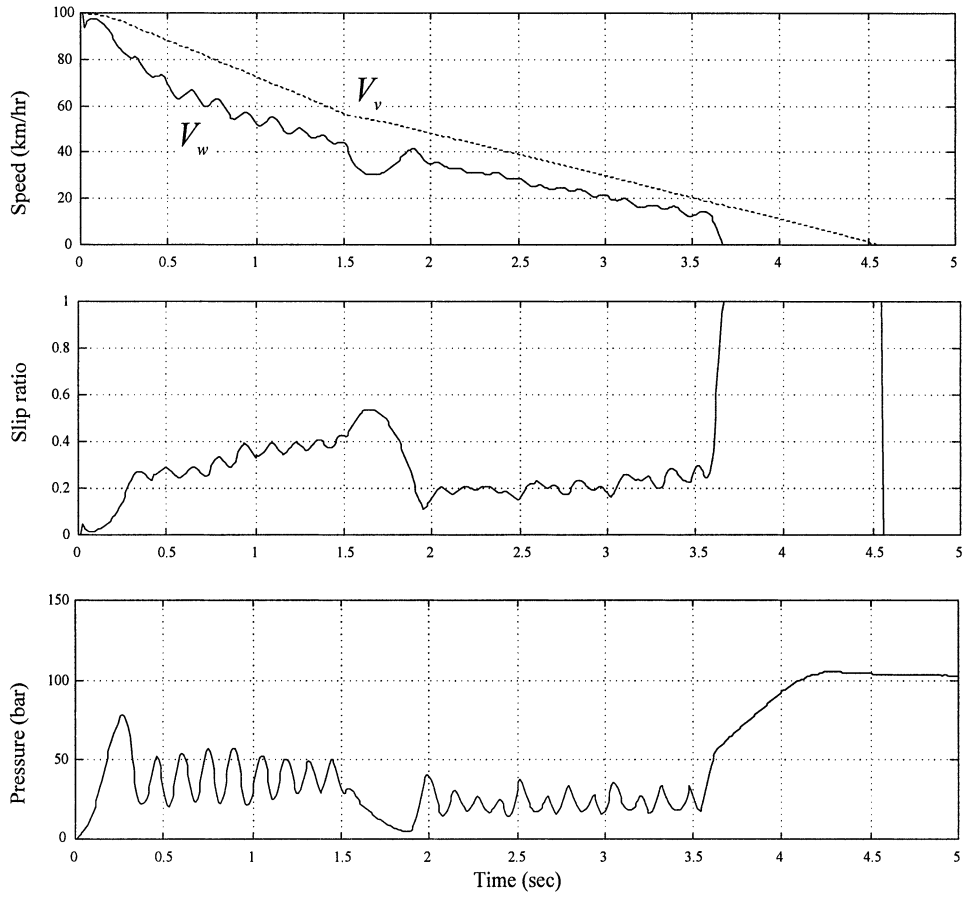

Fig. 14 Results of Fuzzy-PWM control from dry to wet road surface

Table 6 Results without adaptive mechanism

	Brake Time(sec)	Brake Distance(m)	Deceleration(m/s^2)
Dry Road	3.24	47.72	8.57
Wet Road	5.68	82.85	4.89
Dry to Wet	4.60	58.90	6.03
Wet to Dry	3.85	62.56	7.21

Table 7 Results with additional 300 kg weight in vehicle

	Brake Time(sec)	Brake Distance(m)	Deceleration (m/s^2)
Dry Road	3.35	49.78	8.29
Wet Road	5.87	86.37	4.73
Dry to Wet	4.76	62.17	5.83
Wet to Dry	3.98	65.56	7.03

Table 8 Results by conditional on-off control

	Brake Time(sec)	Brake Distance(m)	Deceleration(m/s^2)
Dry Road	3.22	47.17	8.63
Wet Road	5.64	81.76	4.93
Dry to Wet	4.56	58.04	6.09
Wet to Dry	3.83	61.97	7.25

case. On the wet road surface, the distance is even 2 meters longer. The time responses for the dry-to-wet case in Table 6 are shown in Fig. 15 for different road statuses. In this figure, one can see that the amplitude of slip ratio variations becomes higher and more severe; therefore the controller without adaptation cannot track the desired slip ratio as good as the previous one.

5.1.2 Effect of vehicle weight When vehicle weight is increased, there are two different effects on the braking. The first one is that at the same initial speed, more kinetic energy should be transformed to the heat by the brake system before the vehicle stops. However, as the second effect, the normal force on the tire can also be increased to enlarge the adhesion force between tire and road surface. The two factors cause the results to cancel each other. In the experiment, the weight of the vehicle is increased to 1 400 kg (i.e. 300 kg more) while all the other parameters are retained as in Table 3. The same controller with adaptive mechanism is used. The results are shown in Table 7. From the table, one can observe the increase in braking time and distance when compared with the data in Table 5. The 27.3% increase in weight (and kinetic energy) does not increase the distance enormously. It verifies the previous discussion about the two different effects.

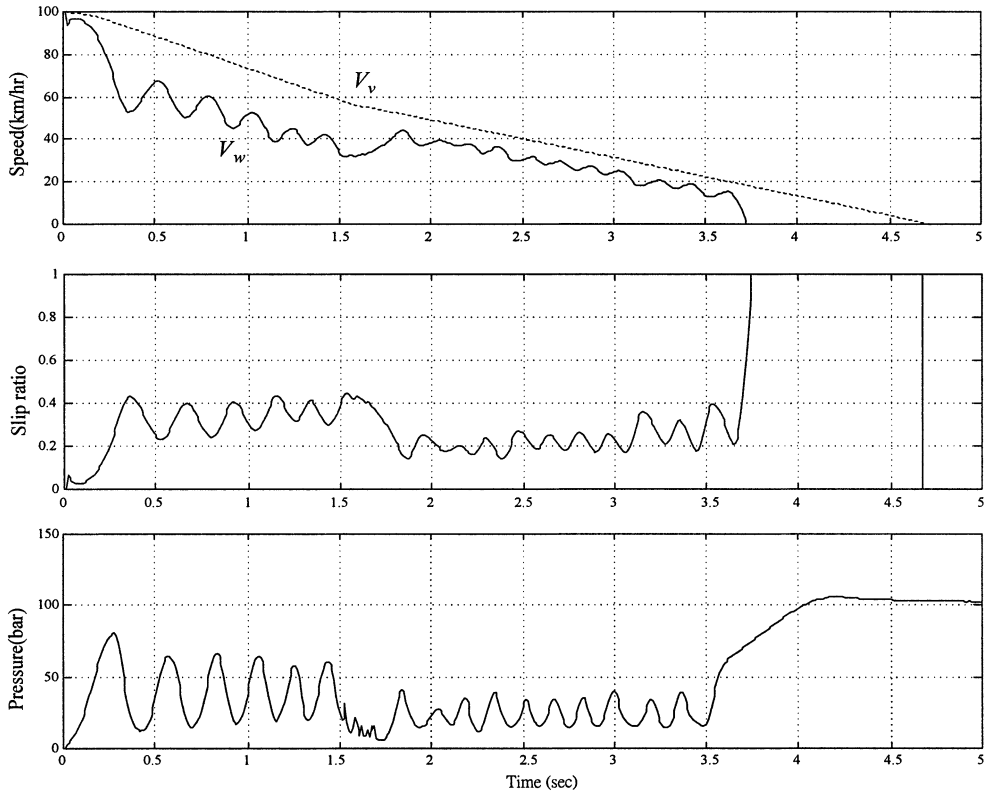

Fig. 15 Results from dry to wet road surface without the adaptive mechanism

5.2 Conditional on-off conversion

In this section, the conditional on-off conversion scheme, as discussed in section 4.4, is used in generating the control signal to the solenoids in ABS module. The three states of the control signal u are I (increase), H (hold) and D (decrease) to control the pressure. In this experiment, the same adaptive PID-type fuzzy control scheme as in section 5.1 and parameters in Table 3 are used, however, the PWM is changed to conditional on-off conversion. Results are shown in Table 8. When compared with Table 5, one can find that the braking distance in Table 8 is longer than that in the PWM case for each corresponding road condition; however, the increased length is less than one meter. Figures 16 and 17 show the time responses of experiments on dry and dry-to-wet surfaces. When compared with the cases in Figs. 13 and 14, one can observe that PWM scheme is better able to track the desired slip ratio. The outcome is not surprising since the PWM scheme can determine the on-off duty ratio in one period while the conditional on-off method maintains the same output during the same period.

6. Conclusion

In this paper, an adaptive PID-type fuzzy controller with on-off conversion is implemented in the application of ABS control. An experimental test bench is built to evaluate the performance of its control results. The result of this ABS control system is obvious and effective for vehicle braking. Two types of on-off conversion schemes, PWM and conditional on-off, are tested and compared by experiments. From the previous discussion, the following results are concluded:

1. The controller with adaptation can track the desired slip ratio better than the one without it. Experiments show that the adaptive mechanism can reduce braking time and distance and improve the braking system's performance.
2. The heavier vehicle has larger normal and friction forces, however, kinetic energy is also proportional to vehicle mass at the same speed. Experiments indicate that the raise in vehicle weight can increase braking distance and time even under the control of ABS system.
3. PWM and conditional on-off conversion schemes are compared in experiments. The PWM conversion shows its superiority to the conditional on-off scheme, since PWM scheme can determine the on-off duty ratio within one sampling period while the other one maintains the same output during the same period.

The controller presented in this study is proved to be effective in tracking the desired the slip ratio and in shortening the braking distance. However, more road testing should be done to take more practical problems into consideration, for example, compensating the yaw moment due to diverse road conditions on four wheels. Also, the load transfer effect that leads to changes in normal forces distribution on front and rear tires may happen in reality.

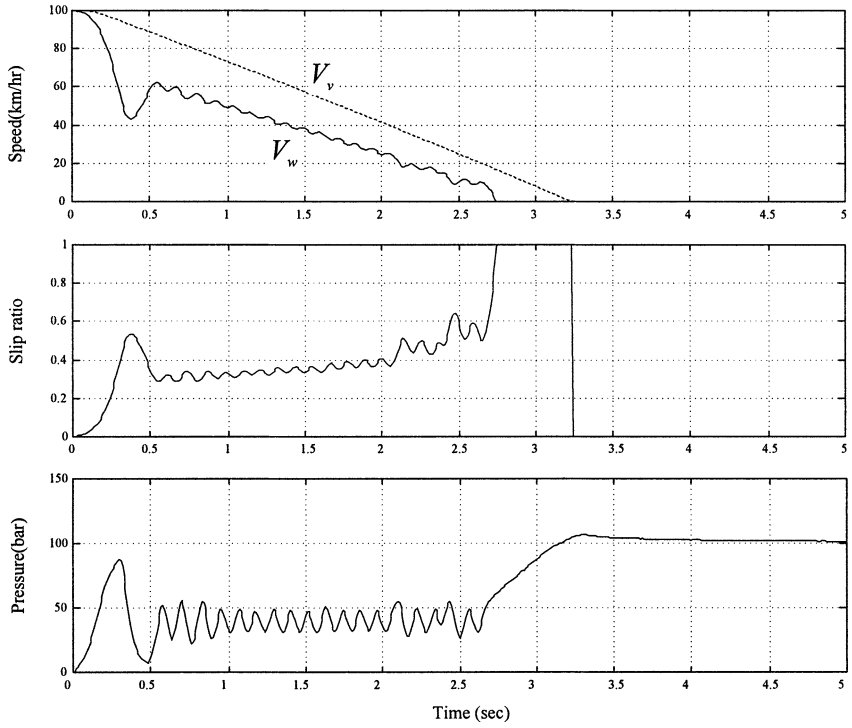

Fig. 16 Results by conditional on-off scheme on dry road surface

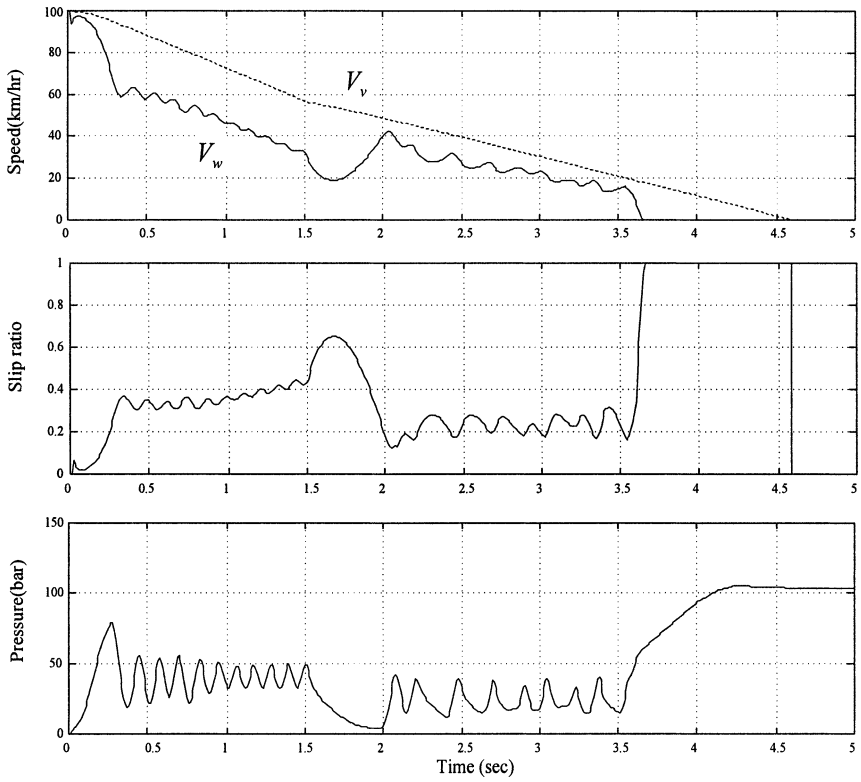

Fig. 17 Results by conditional on-off scheme from dry to wet road surface

These studies need a 2D or even 3D vehicle model to simulate its dynamics during braking. All these should be considered in future research.

References

(1) Bakker, E., Pacejka, H.B. and Lidner, L., A New Tire Model with an Application in Vehicle Dynamics Studies, SAE Paper 890087, (1989).

(2) Chen, C.K. and Wu, J.D., Development of Fuzzy Controlled ABS Systems for Motorcycles, International Journal of Vehicle Design, Vol.34, No.1 (2003), pp.84–100.
(3) Dugoff, H., Fancher, P.S. and Segel, L., An Analysis of Tire Traction Properties and Their Influence on Vehicle Dynamic Performance, SAE Paper, No.700377, (1970).
(4) Fling, R.T. and Fenton, R.E., A Describing-Function Approach to Antiskid Design, IEEE Trans. on Vehicular Technology, Vol.30, No.3 (1981), pp.134–144.
(5) Layne, J.R., Passino, K.M. and Yurkovich, S., Fuzzy Learning Control for Antiskid Braking Systems, IEEE Trans. on Control Systems Technology, Vol.1, No.2 (1993), pp.122–129.
(6) Mauer, G.F., A Fuzzy Logic Controller for an ABS Braking System, IEEE Trans. on Fuzzy System, Vol.3, No.4 (1995), pp.381–388.
(7) McLoughlin, J.H., Limited Slip Braking, Anti-Lock Braking Systems for Road Vehicles, (1985), pp.23–34, ImechE Conference Publications, London, UK.
(8) Qiao, W.Z. and Mizumoto, M., PID Type Fuzzy Controller and Parameters Adaptive Method, Fuzzy Sets and Systems, Vol.78, No.1 (1996), pp.23–35.
(9) Wong, J.Y., Theory of Ground Vehicles, 2nd ed., (1993), John Wiley & Sons, Inc., New York.
(10) Wu, M.C., Lee, L.C. and Shih, M.C., Neuro-Fuzzy Controller Design of the Anti-Lock Braking System, JSME Int. J., Ser. C, Vol.41, No.4 (1998), pp.836–843.
(11) Wu, M.C. and Shih, M.C., Using the Sliding-Mode PWM Method in an Anti-Lock Braking System, Asian Journal of Control, Vol.3, No.3 (2001), pp.255–261.
(12) Wu, M.C. and Shih, M.C., Simulated and Experimental Study of Hydraulic Anti-Lock Braking System Using Sliding-Mode PWM Control, Mechatronics, Vol.13 (2003), pp.331–351.